The fate of standing variation and new mutation under climate change

Cheng-Yueh Lu[1], Cheng-Ruei Lee[1,2,3]*

[1]Institute of Plant Biology, National Taiwan University
[2]Institute of Ecology and Evolutionary Biology, National Taiwan University
[3]Genome and Systems Biology Degree Program, National Taiwan University
*Correspondence to: chengrueilee@ntu.edu.tw

Abstract:
Many species face existence threat under anthropogenic climate change, and standing genetic variation was proposed as a way for sessile species to adapt to novel environments. However, it is still unknown whether standing genetic variants, being adaptive to current environmental variability, are sufficient to guarantee future survival. Here we investigate the relative importance of standing variation versus new mutations and their relative effect sizes from the past to infer the future. While theoretical and experimental evolution studies provided valuable insights, examples in nature are scarce. In the wild banana *Musa itinerans* in Taiwan, we found enrichment of standing variation with environmental associations. New mutations exert larger effect size per variant in precipitation-related climatic variables, where Taiwan contains extreme environments beyond the ancestral climatic range, and novel alleles have stronger association with novel environments. This pattern is reversed for temperature-related variables, where Taiwan is within the ancestral environmental range. Despite such differences, anthropogenic climate change impacts both types of variants strongly. The results constitute one of the few examples in nature demonstrating that the effect sizes of adaptive variants differ under distinct environmental pressures, and the patterns support theoretical predictions that natural selection favors new mutations with larger effect sizes in a novel environment where the population is far from the adaptive peak. Despite the importance of new mutations, however, the pace of anthropogenic climate change may not allow the accumulation of such mutations.

Introduction:

Anthropogenic climatic change posts an imminent threat to most organisms. For large and sessile plant species with long generation time, the speed of migration may not keep up with environmental change, and therefore phenotypic plasticity and genetic variation in the population may allow their survival under novel environments[1-4]. Adaptive genetic variation originates from standing variants before or new mutations after environmental change. Since anthropogenic climate change greatly outpaces natural mutation, the amount of standing genetic variation is therefore critical for the rapid response of a population to changing environments[5-7]. It remains unclear, however, whether standing variants are sufficient to guarantee future survival, given that they are mostly adaptive to the present range of climatic variability. While it may be difficult to perform manipulative experiments in the field to compare the effects of new mutations (NM) and standing variation (SV), one could investigate NM and SV during climatic change in the past.

Adaptation could happen through genetic variants that differ in their origins (NM or SV) or effect sizes (Mendelian genes with major effects or polygenic variants with minor effects). However, how these factors interact and respond to environmental pressures remains relatively uninvestigated. For example, does SV and NM differ in their relative number or effect sizes towards environmental adaptation, and how does this relationship change with different types of environmental factor? For adaptive new mutations that were fixed when facing environment change, Fisher first predicted primarily small allelic effects[8] while Kimura emphasized intermediate effects[9]. Orr, later considering the entire adaptive walk, concluded the evolution towards a novel adaptive peak should first happen through fixation of large-effect mutations and later by small-effect polymorphisms[10]. While this was supported by some studies, the majority of these are microbial experimental evolution in well-controlled environments[11,12], and few have specifically compared the effects of NM and SV. To test whether this idea holds in nature, empirical investigations on natural populations are needed.

Taiwan is well-suited for such studies: Unlike oceanic islands such as Hawaii, Taiwan is a continental island where most species originated from the East Asian continent with recurrent gene flow[13]. The land bridge between Taiwan and China during the glacial maximum allowed exchange of SV, and the isolation during interglacial periods enabled the development of NM. Here we investigate the genomic basis of environmental adaptation of a wild banana species, *Musa itinerans*, whose habitats in Taiwan are considered peripheral from ancestral area reconstructions[14], providing an opportunity to distinguish SV from NM, as well as their response to ancestral versus novel adaptive landscapes. We investigated how past events (SV versus NM) influence present adaptation and whether local adaptation may persist under future anthropogenic climate change.

66 **Results:**

67 **Environmental adaptation in *Musa itinerans***

68 We first sampled *Musa itinerans* at 24 populations across Taiwan (Fig. 1a; Supplementary
69 Fig. 1a; Supplementary Table 1) and investigated the population structure using 14
70 microsatellites (Supplementary Table 2). Environmental Niche Modeling (with 483 occurrence
71 points from field survey and Google Street View) reported species distribution (Fig. 1b) in line
72 with the previous statement that *Musa itinerans* inhabits sunny valleys, watersheds, and
73 hillsides with gentle slopes[15]. Populations differentiated mostly between east and west
74 (Supplementary Fig. 1b). The most unsuitable environments lay within the Central Mountain
75 Range and the southwestern plains (Fig. 1b), respectively corresponding to low annual mean
76 temperature (BIO1) and low precipitation of driest quarter (BIO17), the two most important
77 bioclimatic variables determining species distribution (MaxEnt permutation importance[16]: 36.7
78 for BIO1 and 27.3 for BIO17).

79 To test for local adaptation, we examined the pattern of "isolation by adaptation[17]", a
80 process where differential local adaptation restricted effective gene flow and promoted genetic
81 differentiation among populations, by dissecting geographic and environmental effects on
82 genetic differentiation. The strait-line "fly-over" geographical distance, calculated as the
83 straight-line distance between locations, does not explain patterns of genetic differentiation
84 (Mantel's r = 0.146 and P = 0.062). However, if we considered that Central Mountain Range
85 lacks corridors for *M. itinerans* to disperse (Fig. 1b), this fly-over geographical distance could
86 be too unrealistic. We therefore used resistance distance, calculated from the route with least
87 resistance among populations on the niche suitability map (Fig. 1b), to represent the "realized"
88 geographical distance (Fig. 1c) and found that genetic differentiation was significantly
89 associated with resistance (Mantel's r = 0.226 and P = 0.006). The environmental Mahalanobis
90 distance of bioclimatic variables also showed strong association with genetic differentiation
91 (Mantel's r = 0.298 and P = 0.005). Given that the environmental distance could be strongly
92 dependent on geography, we performed Partial Mantel test to control the geographical effect.
93 After controlling for realized geographic distance (resistance distance), genetic differentiation
94 still correlates with the Mahalanobis environmental distance (Mantel's r = 0.250 and P = 0.012),
95 suggesting differential local adaptation is associated with genetic variation.

96

97 **Standing variation versus new mutations**

98 To identify genomic regions associated with environmental adaptation, we performed
99 pooled sequencing for each population. SNPs were separated into standing variation (SV: both
100 alleles exist in Taiwan and China) or new mutations (NM, polymorphic only in Taiwan). SV
101 outnumbered NM in both adaptive (identified with Bayenv[18]) and non-adaptive SNPs, and after
102 controlling for the overall number of SNPs in SV and NM, SV were further enriched among
103 adaptive polymorphisms (Supplementary Table 3). However, since adaptive SNPs also have

104 higher minor allele frequency (MAF) (Supplementary Fig. 2a), this pattern could be
105 confounded: SV are more likely to have higher MAF than NM, and SNPs with higher MAF
106 may be more likely detected as adaptive due to higher statistical power. We therefore
107 performed the same test with a subset where the adaptive and non-adaptive SNPs have similar
108 allele frequencies (ranging from the first quantile of adaptive MAF to the third quantile of non-
109 adaptive MAF separately for each bioclimatic variable; Supplementary Fig. 2a). In this case as
110 well, SV are still disproportionately abundant (Supplementary Table 4), suggesting SV are
111 more likely than NM to become environment-associated SNPs. Another potential confounding
112 factor is the geographic extent of variants: if most NM resulted from mutations restricted to a
113 few local populations, the limited distribution prevents environment association for NM. We
114 therefore compared the number of Taiwanese populations containing the minor alleles for SV
115 and NM, respectively. Contrary to the direction predicted by the aforementioned confounding
116 factor, the geographic extent of minor alleles for SV is slightly smaller than NM (15.8
117 populations for SV and 16.3 for NM, $P < 0.001$).
118 In addition to SNP number, do NM and SV differ in their directions of effect? Under the
119 null hypothesis that (1) the effects of NM are equally likely to facilitate adaptation to the
120 ancestral or novel environments and (2) natural selection is equally likely to fix NM facilitating
121 adaptation towards either direction, we expected no enrichment of new alleles in either
122 environment. When we separated the Taiwanese populations into those within the Chinese
123 ancestral environmental range and those with novel environments, frequencies of putatively
124 adaptive new alleles in NM SNPs were higher in the latter set of populations, with precipitation
125 of driest quarter (BIO17) and precipitation of coldest quarter (BIO19) showing the strongest
126 effect (Fig. 2a; Supplementary Fig. 2b). Given that the directions of mutation effects should be
127 random, these results suggest that new variants facilitating adaptation to novel environments
128 are more likely to be retained by selection.
129 The results above suggest SV might be more important than NM in terms of enriched
130 number of variants with environment association, and adaptive NM, while lower in number,
131 are more associated with novel environments. On the other hand, the number of candidate SNPs
132 does not necessarily reflect the overall importance of SV over NM, since the effect size also
133 needs to be considered. To investigate the effect size of SV and NM in environmental
134 adaptation, we compared their Bayes factors from Bayenv and focused on two bioclimatic
135 variables that were important in determining species distribution, annual mean temperature
136 (BIO1) and precipitation of driest quarter (BIO17). The two variables exhibit opposite patterns
137 (Fig. 2c): While in BIO17 and other related precipitation variables (Supplementary Fig. 3a)
138 NM consistently had higher Bayes factor and therefore stronger effect size than SV, in BIO1
139 and other related temperature variables (Supplementary Fig. 3a) we observed the reverse. The
140 same trend was observed when we estimated the effect size with gradient forest[19,20] (Fig. 2b, c;
141 Supplementary Fig. 3b, c): BIO17 was the most important factor for differential local

142 adaptation, and NM had stronger effects than SV. On the other hand, BIO1 was the least
143 important factor where SV had stronger effects. Finally, the "importance" estimated by
144 gradient forest is analogous to r^2, representing the amount of allele frequency variation
145 explained by environmental gradients. Assuming a simple linear relationship between allele
146 frequency and environment, the value of r^2 only represents how well each data point (a
147 population) fits along the regression line. We were, however, also interested in the regression
148 slope: the amount of allele frequency changes along environmental gradients (Supplementary
149 Fig. 3d). Again, BIO17 had the largest overall slope among all bioclimatic variables
150 (Supplementary Fig. 3e), with NM being significantly higher than SV (Fig. 2c). BIO1 had the
151 lowest overall slope, again with the reversed pattern. Given that the MAF of adaptive NM and
152 SV SNPs are similar, there is no need to control for allele frequency in these tests
153 (Supplementary Fig. 4a). Therefore, NM with larger effect size per SNP (as estimated by
154 Bayenv Bayes factor, gradient forest r^2 weighted importance, and gradient forest slope) were
155 associated with the adaptation to novel environments outside of the ancestral niche space,
156 consistent with previous population genetics modeling results[8-10].
157 The observed patterns could be integrated with the unique climate of Taiwan. In
158 comparison to the rest of the species range, northern Taiwan experiences northeastern
159 monsoons during winter and has higher precipitation during the typical winter dry season (Fig.
160 3b). This pattern has been maintained since at least the last glacial maximum (Fig. 3d). The
161 novel environments might impose novel adaptive optima to the immigrant population from
162 China. The response to selection imposed by these environmental gradients is strong (with
163 highest Bayes factor, r^2, and slope among all bioclimatic variables; Supplementary Fig. 3a, c,
164 e) especially for NM, where new alleles are strongly associated with novel environments
165 (Supplementary Fig. 2b). More importantly, for this major driver of adaptation (BIO17), the
166 greatest increment of gradient forest importance lies between 200 mm and 300 mm (Fig. 2b),
167 a range also distinguishing the novel Taiwanese versus ancestral Chinese environments (Fig.
168 3b). This suggests that the majority of differential local adaptation is associated with such
169 novel-versus-ancestral environmental differences. Annual mean temperature (BIO1) is the
170 other extreme: the environmental gradient within Taiwan is well within the ancestral Chinese
171 environmental range (Fig. 3a), which can also be traced back to the last glacial maximum (Fig.
172 3c). It is likely that SV already contained genetic variants adaptive to such environmental
173 gradients and are therefore more important than NM (Fig. 2c). In summary, we observed
174 adaptation happening through the assortment of SV for a new territory with similar adaptive
175 landscape and optimum (BIO1; Figs. 2c, 3a, c). For adaptation to novel environments and a
176 new adaptive landscape (BIO17; Figs. 2c, 3b, d), NM with larger effect sizes were more likely
177 favored by natural selection. Our results are therefore consistent with Orr's model[3], providing
178 one of the few examples in nature.

179 One key point of this study is the correct designation of SV or NM. It is possible that some
180 SV SNPs were mis-assigned as NM if we missed an allele in China, most likely for SNPs with
181 low MAF. We addressed this issue with the following: (1) The Taiwanese populations were
182 nested within China in the phylogenetic tree (Supplementary Fig. 4b) and contained much less
183 genetic variation (Supplementary Fig. 4c). Due to the stronger genetic drift in Taiwan than
184 China, it is less likely that an originally SV SNP would retain both alleles in Taiwan but lose
185 one in China. (2) In the extreme case, assuming 50% of NM SNPs were mis-assigned from SV,
186 we performed 100 new analyses, each randomly assigning 50% of NM SNPs back to SV. These
187 new analyses yielded similar results, with NM having higher effect sizes than SV in
188 precipitation-related variables (Supplementary Fig. 5a). (3) Since MAF are correlated between
189 Taiwan and China (Spearman's rank correlation $\rho = 0.35$, $P < 0.001$), we performed analyses
190 with top 50% MAF SNPs in Taiwan, thereby reducing the chance of missing minor alleles in
191 China. The results are qualitatively the same (Supplementary Fig. 5b-d).
192
193 **Fate of adaptive variants under future climate change**
194 In addition to understanding how past events (SV versus NM) affected present adaptation,
195 we are also concerned with how these factors affect the future of this species under
196 anthropogenic climate change. We predicted 16 future outcomes and used Bayenv to
197 investigate the future fate of currently adaptive SNPs. Currently adaptive SNPs retaining high
198 association with future environments are classified as "retention", while those no longer
199 associated with future environments are "disruption". Different from the present pattern of SV
200 being enriched in adaptive SNPs, we saw no clear tendency for any set of adaptive SNPs
201 enriched towards retention or disruption (Supplementary Table 5), suggesting both SV and NM
202 will be affected by climate change.
203 Under the 16 future scenarios we identified two extreme conditions: CCSM4-2070-
204 RCP8.5 as the niche-expansion extreme (Fig. 4a-d) and MIROC-2070-RCP4.5 as the niche-
205 contraction extreme (Fig. 4e-h). Intending to investigate whether SV and NM have different
206 fates under the two contrasting future predictions of this species, we used the genetic offset
207 value from the gradient forest results to estimate genetic mismatch for SV and NM separately,
208 which is associated with the magnitude of allele frequency turnover perturbed by future
209 climatic conditions[20] (Fig. 4b, f). The "genetic offset difference" was calculated by subtracting
210 genetic offset caused by SV from that of NM (Fig. 4c, g). We found no general consensus of
211 whether or where in Taiwan NM or SV SNPs are more affected by climate change (Fig. 4c, g),
212 suggesting NM and SV might both be affected by future anthropogenic climate change despite
213 their distinct genetic architecture in adaptation to current environments.
214 Traditional species distribution models build the species-wide niche model from all
215 occurrence records of a species, thereby assuming all populations in a species reacting equally
216 to the environment and overlooking local adaptation due to within-species polymorphism[6].

Here we propose a concept, "extinction risk", integrating species-level and population-level responses to future climate change simply by dividing genetic offset (estimated from gradient forest) by suitability (estimated from MaxEnt). While the two future conditions exhibit slight differences in suitability and genetic offset, the extinction risks are surprisingly similar, with very high risk in western Taiwan (Fig. 4d, h). In Western Taiwan, the expansion-extreme model suggested high suitability for the species as a whole but also high local population mismatch, thereby having similar trends of extinction risk as the contraction-extreme model. Taken together, our results emphasize the importance of considering both whole-species suitability as well as adaptation of local populations when considering the effect of anthropogenic climate change on the fate of sessile species.

Discussion:

Assessing the within-species variation in climate association is the crucial first step to understand species susceptibility to fluctuating environment, and the relative importance of standing variation (SV) and new mutations (NM) in adaptation has long been debated[7,21-25]. In this study, we investigate how past genetic variation (SV and NM) contribute to the adaptation of present environments as well as how these factors together affect the future fate of a species under anthropogenic climate change.

For a population facing environmental change and therefore a novel adaptive landscape, previous population genetics models have documented the effect size distribution of new mutations fixed by natural selection. Considering the entire adaptive walk of a population facing novel environments, Orr's model predicted the distribution of effect sizes where early substitutions have larger effect than later ones[10]. Consistent with Orr's prediction, we show that NM have stronger effect size than SV in precipitation-related variables, where Taiwan exceeds the ancestral climatic range in China (and therefore the migrating population was far away from the optimum in the new adaptive landscape). This pattern is reversed for temperature-related variables, where Taiwan has similar environmental range as China. Here we provide another perspective to recent research showing that SV contributes to adaptation[7,25]. We show that SV indeed dominate over NM in number[7]. However, the effect size of SV and NM hinges on environmental conditions: natural selection may prefer new mutations contributing to the adaptation to the new rather than the old environment, and the effect sizes of NM tend to be higher than SV under such conditions. Our results imply that standing genetic variation in a population may not be sufficient for the adaptation to anthropogenic climate change.

Ecological niche models are widely used to predict future species distribution, but such models often do not account for the differential adaptation of populations within species. Our observed difference between the major determinant of species-wide range distribution (BIO1) and the driver of differential adaptation of populations within species (BIO17) demonstrates

the need to consider local adaptation. Incorporating species distribution modeling (predicting the future range of the whole species) and genetic offset (predicting the genetic mismatch of each local population to future environments), we identified the potential risk of western lowland populations despite the seemingly distinct species distribution modeling results in different future climate scenarios. In other words, despite in some future scenarios the range of environments suitable for the whole species might increase, giving the impression that the species benefits from anthropogenic climate change, such change might be detrimental to each local population uniquely adapted to a much narrower environmental range than the whole species. Finally, we separately calculated the genetic offset originated from the mismatch of SV or NM to future environments and showed that both will be affected by anthropogenic climate change, regardless of their distinct genetic architecture towards environmental adaptation. Since we distinguished SNPs into SV or NM based on past environmental change, all of these genetic variants will be standing variation when facing future climate change. Novel mutations facilitating the adaptation to new environments may happen in the future, although they will be strongly outpaced by anthropogenic climate change.

Methods:

Sample collection and DNA extraction.

Field work was conducted during 2017 (August - December) and 2018 (January - May). We sampled *Musa itinerans* at 24 sites across Taiwan (Supplementary Fig. 1a; Supplementary Table 1). Fresh leaves were harvested from nine to fifteen individuals at each site. Total genomic DNA was extracted using the standard CTAB extraction method[26]. Since other commercial *Musa* species were also grown in Taiwan, we developed an indel marker for species delimitation. From previous studies[27-30], we identified a 6-bp insertion specific for the Taiwanese *M. itinerans* in the *atpB-rbcL* region of chloroplast. We designed a primer pair (5'-GAAGGGGTAGGATTGATTCTCA-3'; 5'-CGACTTGGCATGGCACTATT-3') and used amplicon size to confirm all collected samples are Taiwanese *M. itinerans*.

Simple sequence repeat genotyping and analysis.

SSR primer sequences used in this study were originally developed for the genus *Musa*[31,32], which were then applied on *Musa itinerans*. Previously documented primer sequences were first searched against the *Musa acuminata* DH-Pahang genome version 2[33] on Banana Genome Hub (https://banana-genome-hub.southgreen.fr/) to check specificity as having only one amplicon, resulting in 26 primer pairs. These primers were then experimented to check specificity on *M. itinerans*, resulting in 14 pairs (Supplementary Table 2). We modified each pair of primers by capping the 5' end of forward primers with M13 sequences (CACGACGTTGTAAAACGAC) and inflorescent molecules[34]. SSR amplicons were run through capillary electrophoresis and the length of each allele was recorded.

293 Population structure of 20 populations (Supplementary Table 1) was analyzed with 14
294 SSR markers (Supplementary Table 2). Lowland populations (C35H, WFL, THNL, PTWT,
295 P199H, MLLYT, HDPG, TTL, NAJY, HLCN, NXIR, and DFR), east transect populations
296 (TPS300, TPS500, TPS700, and TPS900), and west transect populations (XT400, XT700,
297 XT1200, and XT1500) were used in the analysis. We inferred the ancestry of 244 individuals
298 with STRUCTURE 2.3.4[35,36], parameterizing a run to have (1) run length of burnin and after-
299 burnin period of 100,000, (2) admixture ancestry model, and (3) independent allele frequency
300 model, further setting 20 runs for each *K* value.
301 To investigate the association among genetic, geographical, and environmental distance,
302 we generated these distance matrices. Genetic distance was calculated by GenAlEx 6.503[37,38]
303 from 14 SSR markers; straight geographical distance (the fly-over distance) was generated by
304 ArcGIS 10.5 (http://desktop.arcgis.com/en/); environmental distance was measured as
305 Mahalanobis distance to address the correlation among nine bioclimatic variables (below). In
306 addition to the fly-over geographical distance which assumes organism dispersal ignores
307 landscapes, we further calculated as resistance distance the cumulative cost along the least cost
308 path (below). Matrix association was examined under Mantel and Partial Mantel tests.
309 Statistical significance was examined with 1,000 permutations. We performed Mantel tests on
310 (1) genetic distance *vs*. fly-over distance, (2) genetic distance *vs*. resistance distance, (3) genetic
311 distance *vs*. Mahalanobis environmental distance, and Partial Mantel tests on (4) genetic
312 distance *vs*. Mahalanobis environmental distance while controlling for resistance distance.
313
314 **Species distribution modeling.**
315 Current and future species distribution models were built for *Musa itinerans* using
316 presence-only data (483 occurrence points) obtained from field survey and Google Street view.
317 Occurrence points were then reduced to 204 cells by the removal of co-occurring presence data
318 within the same 1×1 km grid. MaxEnt 3.4.1[16], implemented with the maximum entropy
319 modeling approach, reports an overall niche suitability and the importance of predictors by
320 analyzing the presence-only data as well as background (psuedo-absence) data distribution[39-
321 41]. We downloaded from WorldClim database version 1.4 (http://worldclim.org/) spatial layers
322 of 19 present-day bioclimatic variables based on high-resolution monthly temperature and
323 rainfall data[42]. Layers were selected at spatial resolution of 30 arc-second and with a mask that
324 ranges 119.25-122.47°E and 21.76-25.49°N covering Taiwan. Variables showing high
325 dependence (Pearson's correlation coefficient > 0.9 calculated from ENMTools[43]) from each
326 other were removed, resulting in nine final variables: BIO1—mean annual temperature, BIO2
327 —mean diurnal range, BIO3—isothermality, BIO7—temperature annual range, BIO12—
328 annual precipitation, BIO15—precipitation seasonality, BIO16—precipitation of wettest
329 quarter, BIO17—precipitation of driest quarter, and BIO19—precipitation of coldest quarter
330 (Supplementary Table 1).

Present species distribution model was constructed using the default optimization settings in MaxEnt, except the regularization set to three. We tested the predictive model by ten-fold cross-validation which was carried out by randomly partitioning the data into ten equally sized subsets and then replicating models while omitting one subset in turn. In each turn, the predictive model was built using nine subsets as training data and evaluated using the other subset as test data. The output of the predictive model is the probability of presence, or called suitability, and we averaged the ten runs to have an averaged suitability.

To predict the species distribution under different scenarios of future climate change, we projected the present-day model onto eight future climatic conditions combining two periods (2050 and 2070) and four Representative Concentration Pathways (RCP 2.6, RCP 4.5, RCP 6.0, and RCP 8.5). Future climatic layers were obtained from the WorldClim database at spatial resolution of 30 arc-second and were developed based on two general circulation models: the Community Climate System Model[44], CCSM, and the Model for Interdisciplinary Research on Climate[45], MIROC. Species distribution models for the future were carried out using the same settings described above.

To estimate the least cost path between populations, we first generated the resistance surface by taking the reciprocal of suitability. Resistance and suitability is simply a monotonic transformation in which locations with higher suitability exhibit lower resistance. Pairwise least cost path was then measured among 20 populations from the resistance surface, performed by SDM Toolbox v2.3[46]. While least cost path is the single line with least overall cost, we also constructed the least cost corridor between populations, allowing 1%, 2%, or 5% higher cost than the least cost value. In essence, the least cost corridors represent the realized dispersal routes of organisms along suitable habitats.

Sequencing library construction and SNP identification.

We conducted whole genome pooled-sequencing[47] for each population (Supplementary Table 1), resulting in 24 pooled-sequencing libraries. Equal amount of DNA from ten individuals at each population were pooled, except for the PTWT population where only nine individuals were available. A library with 300-400 bp insert size for each pool was prepared using NEBNext Ultra II DNA Library Prep Kit (New England Biolabs). Libraries were then sequenced with 150 bp paired-end on the HiSeq X Ten platform.

Illumina reads were then trimmed with SolexaQA[48], followed by the removal of adaptor sequences with cutadapt[49], subsequently mapped to the *Musa itinerans* reference genome assembly ASM164941v1[50] with BWA 0.7.15[51]. Picard Tools (http://broadinstitute.github.io/picard) was used to mark duplicated read pairs, and the genotypes were called following GATK 3.7 best practice[52].

For the 24 pooled samples, we filtered out sites with (1) more than two alleles, (2) indels, (3) quality (QUAL) < 30, (4) quality by depth (QD) < 2, (5) call rate < 0.74, and (6) depth (DP)

369 > genome-wide average depth plus three standard deviations, resulting in 4,200,177 SNPs.
370 SNPs with (1) minor allele frequency (MAF) < 0.05, (2) missing data in any of the pooled-seq
371 sample, and (3) DP per sample < 20 were further filtered out, resulting in 1,256,894 SNPs.
372 To investigate the relationship between Taiwanese and Chinese *M. itinerans*, we
373 downloaded public data from 24 Chinese accessions (SRR6382516 - SRR6382539)[53]. SNPs
374 were called using all 24 Chinese and the 24 Taiwanese samples together following the pipeline
375 described above. We did not perform any site filtering for this joint data set since the main
376 objective is to investigate whether specific SNPs in Taiwan also existed in China as SV. This
377 dataset has 18,442,853 SNPs. SRR6382532 was excluded due to high missing rate. Only when
378 evaluating the averaged expected heterozygosity between Taiwanese and Chinese populations
379 did we filter out sites with (1) indels and (2) QUAL < 30, resulting in 15,591,923 SNPs.
380 To assess the phylogeny of our Taiwanese populations and Chinese accessions, we
381 downloaded *Musa acuminata* sequence (SRR7013754) as an outgroup. SNPs were called using
382 one *M. acuminata* species, 24 Chinese and 24 Taiwanese samples together following the
383 pipeline described above. We filtered out sites with (1) more than two alleles, (2) indels, (3)
384 QUAL < 30, and (4) call rate < 0.9, resulting in 12,693,687 SNPs. This dataset also excluded
385 SRR6382532.
386
387 **Environmentally-associated SNP identification.**
388 We used Bayenv 2.0[18] to search for SNPs highly associated with environmental variables.
389 Bayenv estimates the relationship between SNPs and environments while controlling the
390 whole-genome population structure from a subset of loose linkage-disequilibrium SNPs. Loose
391 linkage-disequilibrium SNPs were formed by sampling (1) one SNP from scaffolds more than
392 10 kb and less than 100 kb, (2) two SNPs from scaffolds more than 100 kb and less than 500
393 kb, (3) three SNPs from scaffolds more than 500 kb and less than 1000 kb, and (4) four SNPs
394 from scaffolds more than 1000 kb. We then, for each bioclimatic variable, defined as the
395 adaptive SNPs ones exhibiting top 1% Bayes factor and top 5% rho value (a nonparametric
396 correlation coefficient capable to reduce outlier effects).
397 We further investigated the fate of currently adaptive SNPs under anthropogenic climate
398 change, performing the same Bayenv analyses of currently adaptive SNPs using future climatic
399 conditions. We included two time periods (2050 and 2070) and four Representative
400 Concentration Pathways (RCP 2.6, RCP 4.5, RCP 6.0, and RCP 8.5) from two general
401 circulation models, CCSM[44] and MIROC[45], resulting in 16 future climatic conditions. If a
402 currently adaptive SNP remains strongly associated with environments, it should exhibit Bayes
403 factor above the current threshold. We then defined as "retention" a currently adaptive SNP
404 constantly exhibiting Bayes factor above the current adaptive threshold in all future scenarios,
405 and defined as "disruption" a currently adaptive SNP exhibiting Bayes factor above the current
406 adaptive threshold in none of the future scenarios.

The gradient forest method and genetic offset.

We used a novel method, gradient forest[19,20], to estimate the effect of environmental gradients on allele frequency differences among populations. Gradient forest is a regression-tree based machine-learning algorithm using environmental variables to partition SNP allele frequencies. The analysis was done separately for each SNP. The resulting "importance" measures how much of the variation in allele frequency was explained by partitioning the populations based on a specific value in an environmental variable. By making multiple regression trees (thus generating a random forest) for a SNP, the goodness-of-fit r^2 of a random forest is measured as the proportion of variance explained by this random forest, which is then partitioned among environmental variables in proportion to their conditional importance. Such SNP-wise importance of each environmental variable is then averaged across SNPs belonging to the standing variation (SV) or new mutations (NM) group, resulting in the overall importance (of each environmental variable). In the end, one could obtain the relation curve between environmental gradient and cumulative importance (analogous to the cumulative r^2, proportion of allele frequency differences among populations explained by environments). This curve has two properties. First, the highest point of the cumulative importance curve denotes the overall association between a climatic variable and allele frequency, and we used this to represent the effect size of these SNPs. Second, when traversing along the environmental gradient, a sudden increase of cumulative importance at some environmental value (for example, 20°C) denotes populations on either side of this environmental cutoff have very different allele frequency compositions. In other words, this represents a threshold factor for local adaptation.

One can use this cumulative importance curve to estimate the effect of future environmental change on local populations. In the example above, a population's local temperature increased from 19°C to 21°C due to climate change would require larger allele frequency shift than another population whose local temperature changed from 17°C to 19°C. The "genetic offset"[10] could then be calculated as the Euclidean distance between cumulative importance corresponding to the contemporary environmental value and that corresponding to the future environmental value, considering all bioclimatic variables together. Genetic offset can then be considered to be the magnitude of genetic change needed for a population to be still adaptive in the face of climate change.

Regression slope.

The regression slope is not given by gradient forest, since it only reports the r^2 importance estimate. Thus, we introduced the simple linear regression $y=\alpha+\beta x$ to measure the regression slope. We took y as the allele frequency, x as the standardized bioclimatic variable, and β (slope) as the measurement of the amount of allele frequency changes along environmental gradients. By fitting simple linear regression with the general least-square approach, β can

then be expanded to $r_{xy}\frac{s_y}{s_x}$, where r_{xy} is the correlation coefficient (the square root of gradient forest measured "importance") between x (environment value) and y (allele frequency), and s_x and s_y are the standard deviation of x and y.

References:

1 Bradshaw, A. D. Evolutionary significance of phenotypic plasticity in plants. in *Advances in Genetics* **13** (eds Caspari, E. W. & Thoday, J. M.) 115-155 (Academic Press, 1965).

2 Ghalambor, C. K., McKay, J. K., Carroll, S. P. & Reznick, D. N. Adaptive versus non-adaptive phenotypic plasticity and the potential for contemporary adaptation in new environments. *Funct. Ecol.* **21**, 394-407, doi:10.1111/j.1365-2435.2007.01283.x (2007).

3 Jump, A. S. & Peñuelas, J. Running to stand still: adaptation and the response of plants to rapid climate change. *Ecol. Lett.* **8**, 1010-1020, doi:10.1111/j.1461-0248.2005.00796.x (2005).

4 Franks, S. J., Weber, J. J. & Aitken, S. N. Evolutionary and plastic responses to climate change in terrestrial plant populations. *Evol. Appl.* **7**, 123-139, doi:10.1111/eva.12112 (2014).

5 Barrett, R. D. H. & Schluter, D. Adaptation from standing genetic variation. *Trends Ecol. Evol.* **23**, 38-44, doi:10.1016/j.tree.2007.09.008 (2008).

6 Razgour, O. *et al.* Considering adaptive genetic variation in climate change vulnerability assessment reduces species range loss projections. *Proc. Natl. Acad. Sci. USA* **116**, 10418-10423, doi:10.1073/pnas.1820663116 (2019).

7 Lai, Y. T. *et al.* Standing genetic variation as the predominant source for adaptation of a songbird. *Proc. Natl. Acad. Sci. USA* **116**, 2152-2157, doi:10.1073/pnas.1813597116 (2019).

8 Fisher, R. A. *The Genetical Theory of Natural Selection*. (Clarendon Press, Oxford, England, 1930).

9 Kimura, M. *The Neutral Theory of Molecular Evolution*. (Cambridge University Press, Cambridge, England, 1983).

10 Orr, H. A. The population genetics of adaptation: The distribution of factors fixed during adaptive evolution. *Evolution* **52**, 935-949, doi:10.2307/2411226 (1998).

11 Barrick, J. E. *et al.* Genome evolution and adaptation in a long-term experiment with *Escherichia coli. Nature* **461**, 1243-1247, doi:10.1038/nature08480 (2009).

12 Gifford, D. R., Schoustra, S. E. & Kassen, R. The length of adaptive walks is insensitive to starting fitness in *Aspergillus nidulans*. *Evolution* **65**, 3070-3078, doi:10.1111/j.1558-5646.2011.01380.x (2011).

13 Bramwell, D. & Caujapé-Castells, J. *The Biology of Island Floras*. (Cambridge University Press, Cambridge, 2011).

14 Janssens, S. B. *et al.* Evolutionary dynamics and biogeography of Musaceae reveal a correlation between the diversification of the banana family and the geological and climatic history of Southeast Asia. *New Phytol.* **210**, 1453-1465,

487 doi:10.1111/nph.13856 (2016).
488 15 Chiu, H. L. The collection, evaluation and analysis of genetic diversity of *Musa*
489 *formosana* (Warb.) Hayata native in Taiwan. (National Taiwan University, 2004).
490 16 Phillips, S. J., Anderson, R. P. & Schapire, R. E. Maximum entropy modeling of
491 species geographic distributions. *Ecol. Model.* **190**, 231-259,
492 doi:10.1016/j.ecolmodel.2005.03.026 (2006).
493 17 Nosil, P., Egan, S. P. & Funk, D. J. Heterogeneous genomic differentiation between
494 walking-stick ecotypes: "isolation by adaptation" and multiple roles for divergent
495 selection. *Evolution* **62**, 316-336, doi:10.1111/j.1558-5646.2007.00299.x (2008).
496 18 Gunther, T. & Coop, G. Robust identification of local adaptation from allele
497 frequencies. *Genetics* **195**, 205-220, doi:10.1534/genetics.113.152462 (2013).
498 19 Ellis, N., Smith, S. J. & Pitcher, C. R. Gradient forests: calculating importance
499 gradients on physical predictors. *Ecology* **93**, 156-168, doi:10.1890/11-0252.1 (2012).
500 20 Fitzpatrick, M. C. & Keller, S. R. Ecological genomics meets community-level
501 modelling of biodiversity: mapping the genomic landscape of current and future
502 environmental adaptation. *Ecol. Lett.* **18**, 1-16, doi:10.1111/ele.12376 (2015).
503 21 Barton, N. H. Genetic hitchhiking. *Philos. Trans. R. Soc. Lond. Ser. B-Biol. Sci.* **355**,
504 1553-1562, doi:10.1098/rstb.2000.0716 (2000).
505 22 Linnen, C. R., Kingsley, E. P., Jensen, J. D. & Hoekstra, H. E. On the origin and
506 spread of an adaptive allele in deer mice. *Science* **325**, 1095-1098,
507 doi:10.1126/science.1175826 (2009).
508 23 Jones, F. C. *et al.* The genomic basis of adaptive evolution in threespine sticklebacks.
509 *Nature* **484**, 55-61, doi:10.1038/nature10944 (2012).
510 24 Reid, N. M. *et al.* The genomic landscape of rapid repeated evolutionary adaptation to
511 toxic pollution in wild fish. *Science* **354**, 1305-1308, doi:10.1126/science.aah4993
512 (2016).
513 25 Ahrens, C. W., Byrne, M. & Rymer, P. D. Standing genomic variation within coding
514 and regulatory regions contributes to the adaptive capacity to climate in a foundation
515 tree species. *Mol. Ecol.* **28**, 2502-2516, doi:10.1111/mec.15092 (2019).
516 26 Doyle, J. J. & Doyle, J. L. A rapid DNA isolation procedure for small quantities of
517 fresh leaf tissue. *Phytochemical Bulletin* **19,** 11-15 (1987).
518 27 White, T. J., Bruns, T., Lee, S. & Taylor, J. Amplification and direct sequencing of
519 fungal ribosomal RNA genes for phylogenetics. in *PCR Protocols* (eds Innis, M. A.,
520 Gelfand, D. H., Sninsky, J. J. & White, T. J.) 315-322 (Academic Press, San Diego,
521 California, 1990).
522 28 Taberlet, P., Gielly, L., Pautou, G. & Bouvet, J. Universal primers for amplification of
523 three non-coding regions of chloroplast DNA. *Plant Mol. Biol.* **17**, 1105-1109,
524 doi:10.1007/BF00037152 (1991).

29 Oxelman, B., Lidén, M. & Berglund, D. Chloroplast *rps16* intron phylogeny of the tribe Sileneae (Caryophyllaceae). *Plant Syst. Evol.* **206**, 393-410, doi:10.1007/BF00987959 (1997).

30 Hurr, K. A., Lockhart, P. J., Heenan, P. B. & Penny, D. Evidence for the recent dispersal of *Sophora* (Leguminosae) around the Southern Oceans: molecular data. *J. Biogeogr.* **26**, 565-577, doi:10.1046/j.1365-2699.1999.00302.x (1999).

31 Lagoda, P. J. *et al.* Sequence tagged microsatellite site (STMS) markers in the Musaceae. *Mol. Ecol.* **7**, 659-663 (1998).

32 Crouch, H. K., Crouch, J. H., Jarret, R. L., Cregan, P. B. & Ortiz, R. Segregation at microsatellite loci in haploid and diploid gametes of *Musa*. *Crop Sci.* **38**, 211-217, doi:10.2135/cropsci1998.0011183X003800010035x (1998).

33 Martin, G. *et al.* Improvement of the banana "*Musa acuminata*" reference sequence using NGS data and semi-automated bioinformatics methods. *BMC Genomics* **17**, 243, doi:10.1186/s12864-016-2579-4 (2016).

34 Schuelke, M. An economic method for the fluorescent labeling of PCR fragments. *Nat. Biotechnol.* **18**, 233-234, doi:10.1038/72708 (2000).

35 Pritchard, J. K., Stephens, M. & Donnelly, P. Inference of population structure using multilocus genotype data. *Genetics* **155**, 945-959 (2000).

36 Falush, D., Stephens, M. & Pritchard, J. K. Inference of population structure using multilocus genotype data: linked loci and correlated allele frequencies. *Genetics* **164**, 1567-1587 (2003).

37 Peakall, R. O. D. & Smouse, P. E. Genalex 6: genetic analysis in Excel. Population genetic software for teaching and research. *Mol. Ecol. Notes* **6**, 288-295, doi:10.1111/j.1471-8286.2005.01155.x (2006).

38 Peakall, R. & Smouse, P. E. GenAlEx 6.5: genetic analysis in Excel. Population genetic software for teaching and research--an update. *Bioinformatics* **28**, 2537-2539, doi:10.1093/bioinformatics/bts460 (2012).

39 Bean, W. T., Stafford, R. & Brashares, J. S. The effects of small sample size and sample bias on threshold selection and accuracy assessment of species distribution models. *Ecography* **35**, 250-258, doi:10.1111/j.1600-0587.2011.06545.x (2012).

40 Elith, J. *et al.* Novel methods improve prediction of species' distributions from occurrence data. *Ecography* **29**, 129-151, doi:10.1111/j.2006.0906-7590.04596.x (2006).

41 Elith, J. *et al.* A statistical explanation of MaxEnt for ecologists. *Divers. Distrib.* **17**, 43-57, doi:10.1111/j.1472-4642.2010.00725.x (2011).

42 Hijmans, R. J., Cameron, S. E., Parra, J. L., Jones, P. G. & Jarvis, A. Very high resolution interpolated climate surfaces for global land areas. *Int. J. Climatol.* **25**, 1965-1978, doi:10.1002/joc.1276 (2005).

43 Warren, D. L., Glor, R. E. & Turelli, M. ENMTools: a toolbox for comparative studies of environmental niche models. *Ecography* **33**, 607-611, doi:10.1111/j.1600-0587.2009.06142.x (2010).

44 Gent, P. R. *et al.* The Community Climate System Model Version 4. *J. Climate* **24**, 4973-4991, doi:10.1175/2011jcli4083.1 (2011).

45 Watanabe, S. *et al.* MIROC-ESM 2010: model description and basic results of CMIP5-20c3m experiments. *Geosci. Model Dev.* **4**, 845-872, doi:10.5194/gmd-4-845-2011 (2011).

46 Brown, J. L. & Anderson, B. SDMtoolbox: a python-based GIS toolkit for landscape genetic, biogeographic and species distribution model analyses. *Methods Ecol. Evol.* **5**, 694-700, doi:10.1111/2041-210x.12200 (2014).

47 Schlotterer, C., Tobler, R., Kofler, R. & Nolte, V. Sequencing pools of individuals - mining genome-wide polymorphism data without big funding. *Nat. Rev. Genet.* **15**, 749-763, doi:10.1038/nrg3803 (2014).

48 Cox, M. P., Peterson, D. A. & Biggs, P. J. SolexaQA: At-a-glance quality assessment of Illumina second-generation sequencing data. *BMC Bioinformatics* **11**, 485, doi:10.1186/1471-2105-11-485 (2010).

49 Martin, M. Cutadapt removes adapter sequences from high-throughput sequencing reads. *EMBnet.journal* **17**, 10-12, doi:10.14806/ej.17.1.200 (2011).

50 Wu, W. *et al.* Whole genome sequencing of a banana wild relative *Musa itinerans* provides insights into lineage-specific diversification of the *Musa* genus. *Sci. Rep.* **6**, 31586, doi:10.1038/srep31586 (2016).

51 Li, H. & Durbin, R. Fast and accurate short read alignment with Burrows-Wheeler transform. *Bioinformatics* **25**, 1754-1760, doi:10.1093/bioinformatics/btp324 (2009).

52 McKenna, A. *et al.* The Genome Analysis Toolkit: A MapReduce framework for analyzing next-generation DNA sequencing data. *Genome Res.* **20**, 1297-1303, doi:10.1101/gr.107524.110 (2010).

53 Wu, W., Ng, W. L., Yang, J. X., Li, W. M. & Ge, X. J. High cryptic species diversity is revealed by genome-wide polymorphisms in a wild relative of banana, *Musa itinerans*, and implications for its conservation in subtropical China. *BMC Plant Biol.* **18**, 194, doi:10.1186/s12870-018-1410-6 (2018).

Figures:

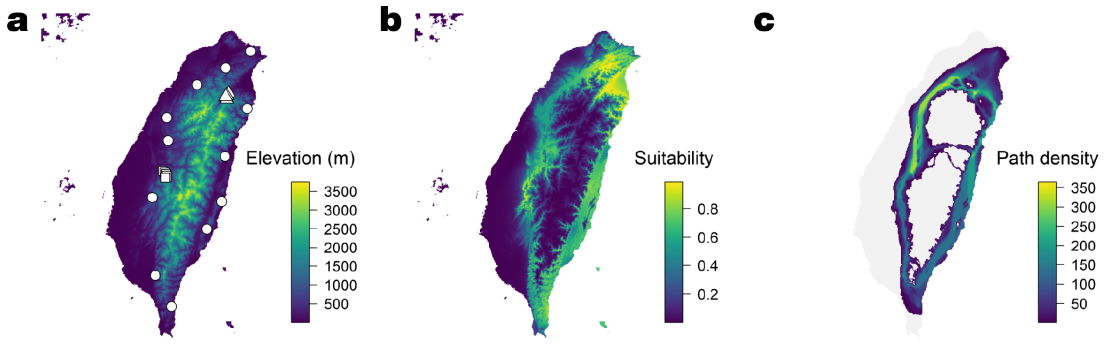

Fig. 1 | Sample distribution and niche modeling of *Musa itinerans*. a, Sampling sites are distributed along the latitudinal and altitudinal gradient. Lowland populations are represented as white circles; transect populations are represented as white triangles and squares. **b**, Suitability is derived from MaxEnt niche modeling. **c**, Least-cost-corridor landscape is constructed from pairwise least-cost paths among 20 populations from the resistance surface (the reciprocal of niche suitability).

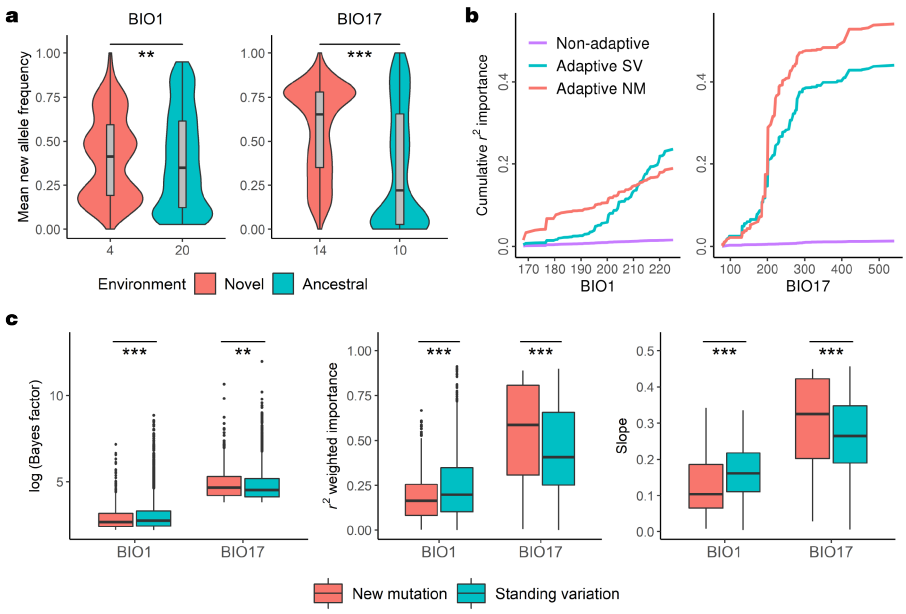

Fig. 2 | The environment-dependent enrichment of new alleles and the distinct effect sizes of standing variation (SV) and new mutations (NM) in contrasting climatic factors. BIO1 reflects annual mean temperature, and BIO17 indicates precipitation of driest quarter. **a**, Mean frequency of new alleles among NM SNPs compared between populations that have local environments within or outside of the ancestral climatic range. New alleles are enriched in novel environments (**$P < 0.01$, ***$P < 0.001$, *t*-test). Values on the horizontal axis denote the number of Taiwanese populations within the ancestral or novel environmental range. **b**, Gradient forest cumulative r^2 importance is shown along environmental gradients. **c**, Effect sizes as estimated from Bayes factor, gradient forest r^2 importance, and gradient forest slope all show that SV exhibit higher effect sizes in BIO1 but the reverse in BIO17 (**$P < 0.01$, ***$P < 0.001$, Wilcoxon rank-sum test for Bayes factor and *t*-test for r^2 importance and slope).

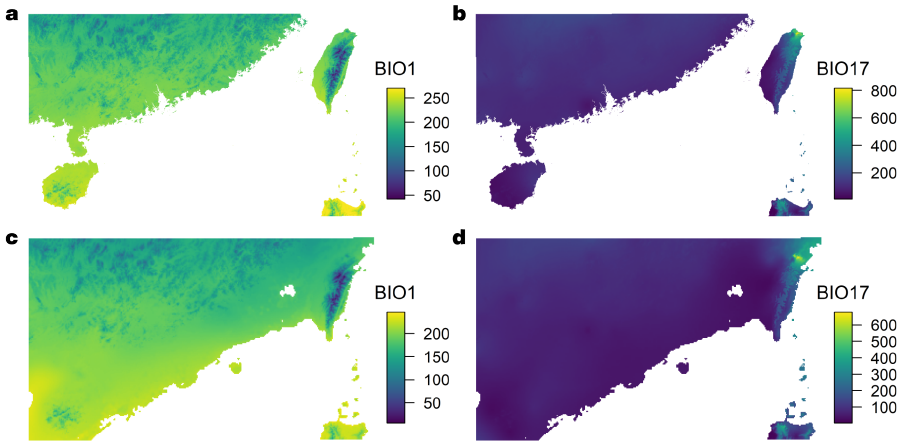

Fig. 3 | Annual mean temperature (BIO1) and precipitation of driest quarter (BIO17) for the present and last glacial maximum. a, **b**, Present environments. **c**, **d**, Last-glacial-maximum environments, showing the environments on the extent of land. Maps on all panels have the same range in latitude and longitude.

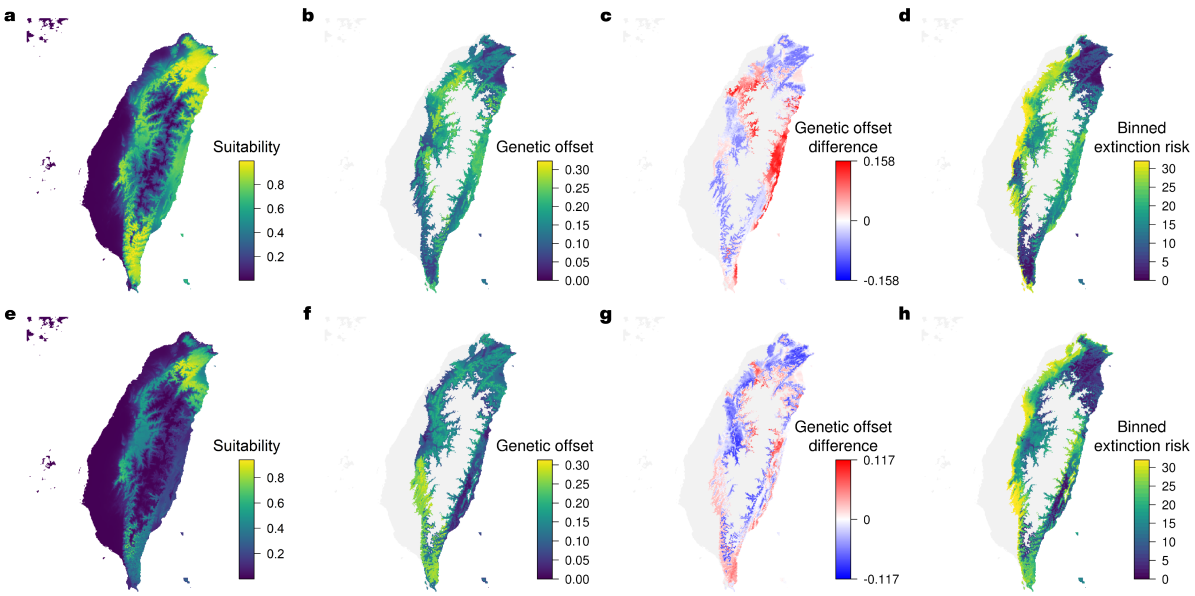

Fig. 4 | The fate of *Musa itinerans* under two extreme future conditions. a-d, Niche-expansion extreme (CCSM4-2070-RCP8.5) reports the species-average niche suitability from MaxEnt modeling (**a**), the genetic mismatch of locally adaptive populations to future environments based on the genetic offset from gradient forest (**b**), genetic offset difference calculated as the genetic offset experienced by new mutations minus that from standing variation (**c**), and extinction risk estimated as genetic offset divided by niche suitability (shown as 32 bins with equal grid counts; **d**). **e-h**, Niche-contraction extreme (MIROC-2070-RCP4.5) reports the suitability (**e**), genetic offset (**f**), genetic offset difference (**g**), and extinction risk (**h**). Grids with present niche suitability < 0.2 are excluded and colored in gray in **b-d** and **f-h**.

Data Availability:

Population pooled sequencing reads are available under NCBI BioProject PRJNA575344.

Acknowledgements:

We thank Thomas Mitchell-Olds for valuable comments, Hui-Long Chiu for the knowledge of *Musa itinerans* ecology in Taiwan, Chia-Yu Chen, Zhe-Ting Kuo, and Jo-Wei Hsieh for the assistance of sample preparation, Hao-Chih Kuo for the introduction to species distribution modeling, Cheng-Tao Lin for providing the R template of some maps, the Lee lab member for valuable discussions, and the Computer and Information Networking Center of National Taiwan University for the support of high-performance computing facilities. This work is supported by the Ministry of Science and Technology of Taiwan (106-2628-B-002-001-MY3, 107-2636-B-002-004, and 108-2636-B-002-004 to CRL).

Author Contributions:

C-RL designed the research. Both authors performed experiments and analyses and wrote the manuscript.

Competing Interest Declaration:

None

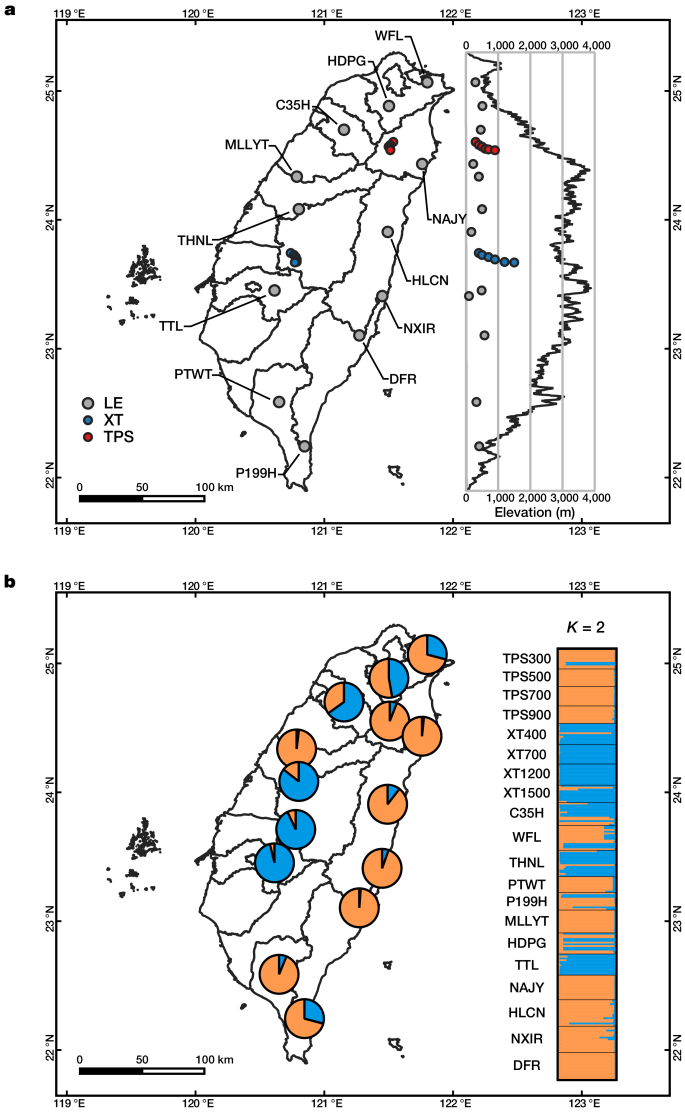

Supplementary Fig. 1 | Sampling site and population structure of Taiwanese *Musa itinerans* under STRUCTURE *K* = 2. a, Solid circles represent collection locations corresponding to their coordinates and elevation: Gray circles indicate populations of low elevation (LE); blue circles indicate populations of Xitou transect (XT); red circles indicate populations of Taipingshan transect (TPS). **b**, Individual ancestry is plotted on the right side, while population ancestry is plotted on map with a pie chart. Map template is provided by *Cheng-Tao Lin.

*Cheng-Tao Lin (2018) QGIS template for displaying species distribution by horizontal and vertical view in Taiwan. URL: https://github.com/mutolisp/distrmap_tw.qgis. DOI: 10.5281/zenodo.1493690

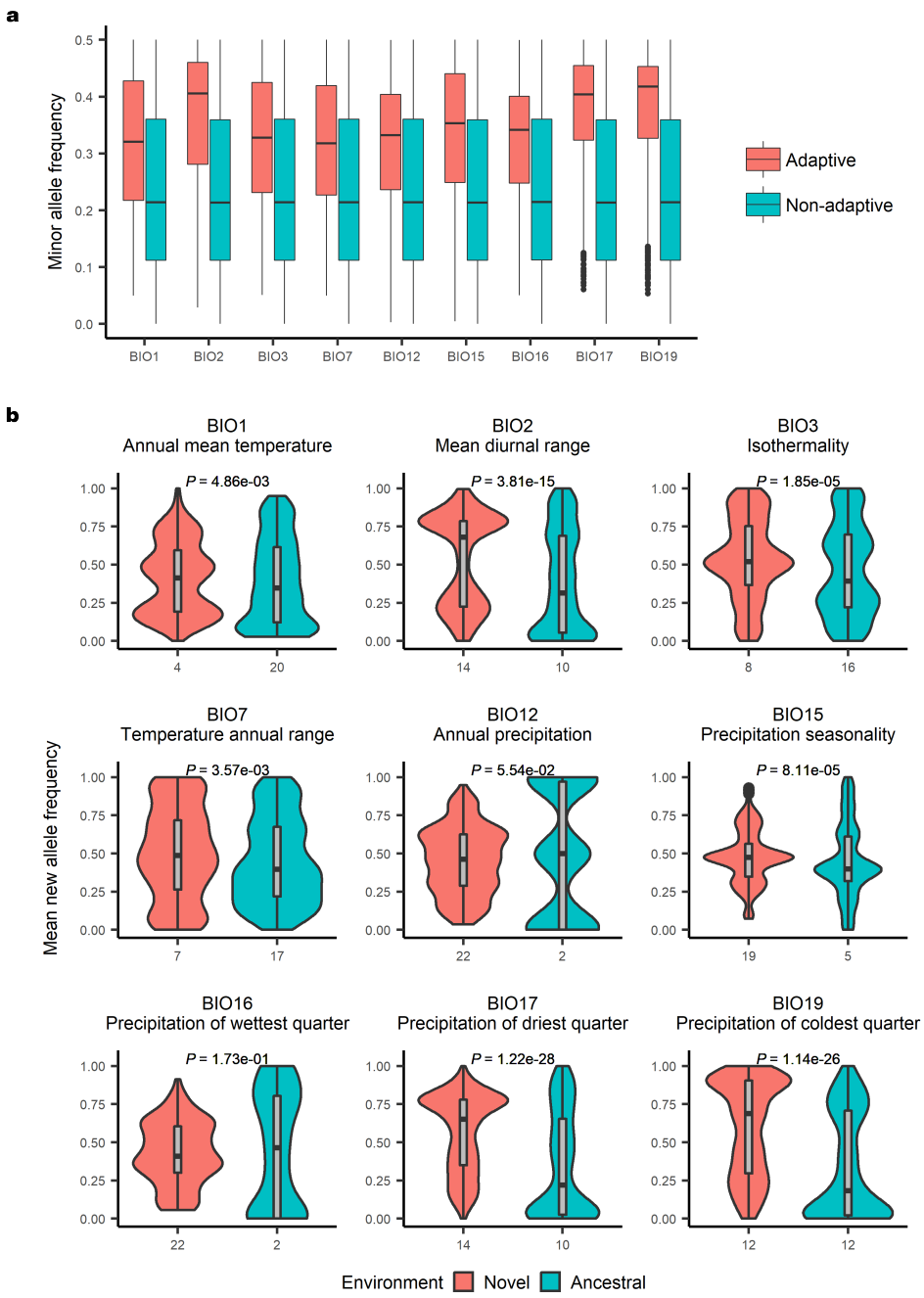

Supplementary Fig. 2 | Allele frequency distribution. a, Minor allele frequency distribution of adaptive and non-adaptive SNPs. **b**, Frequency of new alleles in Taiwanese populations within the ancestral or novel environmental range. Statistical significance from Student's *t*-test between the novel and ancestral environmental range for each bioclimatic variable is shown. Values on the horizontal axis denote the number of Taiwanese populations within the ancestral or novel environmental range.

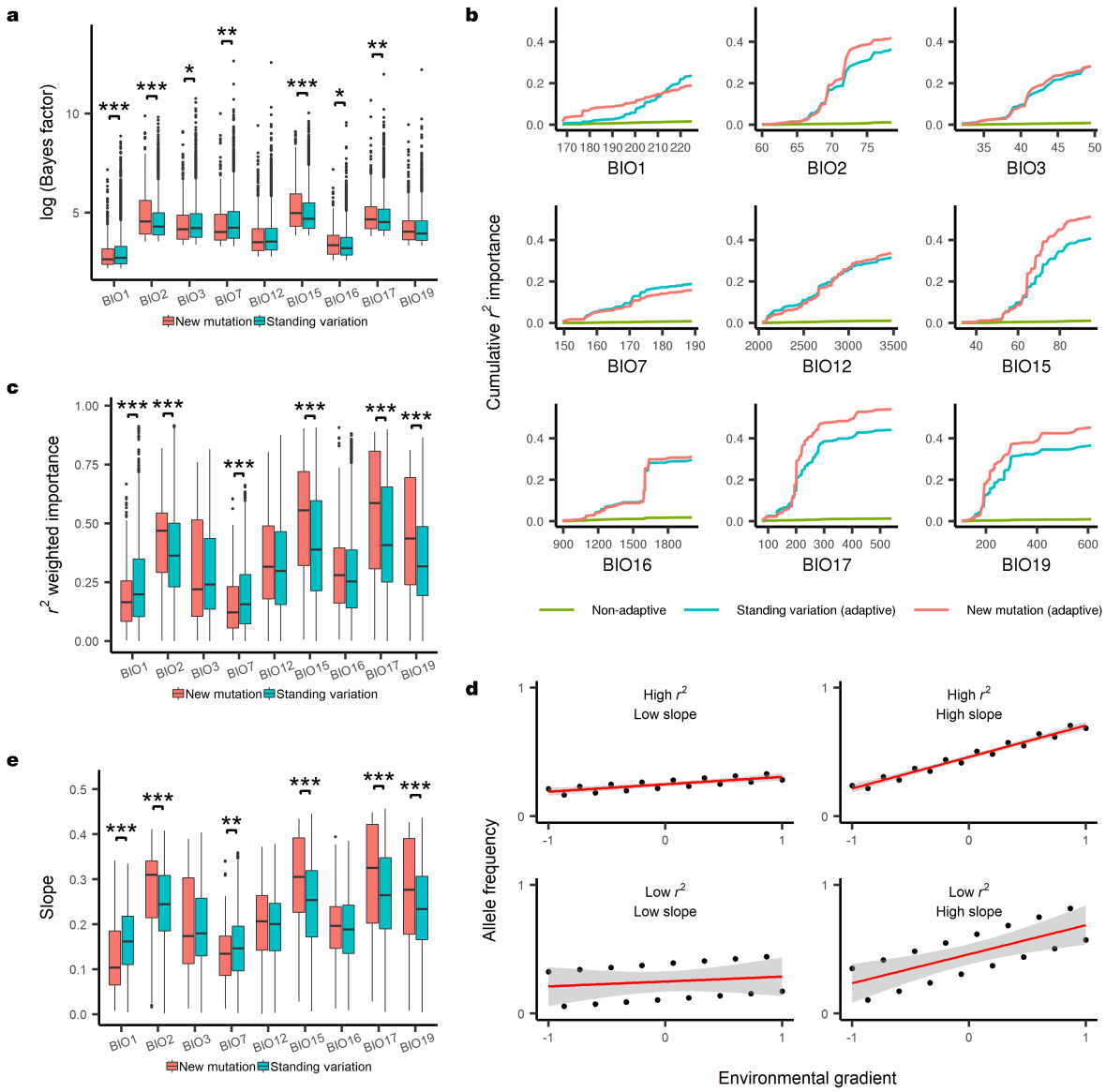

Supplementary Fig. 3 | Profiling of effect sizes. a, Bayenv Bayes factor distribution for adaptive new mutations and standing variation (*$P < 0.05$, **$P < 0.01$, ***$P < 0.001$, Wilcoxon rank-sum test). **b**, Cumulative r^2 importance from gradient forest along environmental gradients. **c**, Gradient forest r^2 importance distribution (***$P < 0.001$, Welch's *t*-test). **d**, Example figure showing the relationship between r^2 importance and slope. r^2 indicates the extent that allele frequency fits a linear model, while slope indicates the amount of allele frequency changes along the linear relationship. The graphs indicate one should also investigate regression slopes in addition to the gradient forest r^2. Values on the horizontal axis show the range of standardized environmental variables. **e**, The distribution of regression slopes when one regresses adaptive SNP allele frequency onto environmental gradients (**$P < 0.01$, ***$P < 0.001$, Welch's *t*-test).

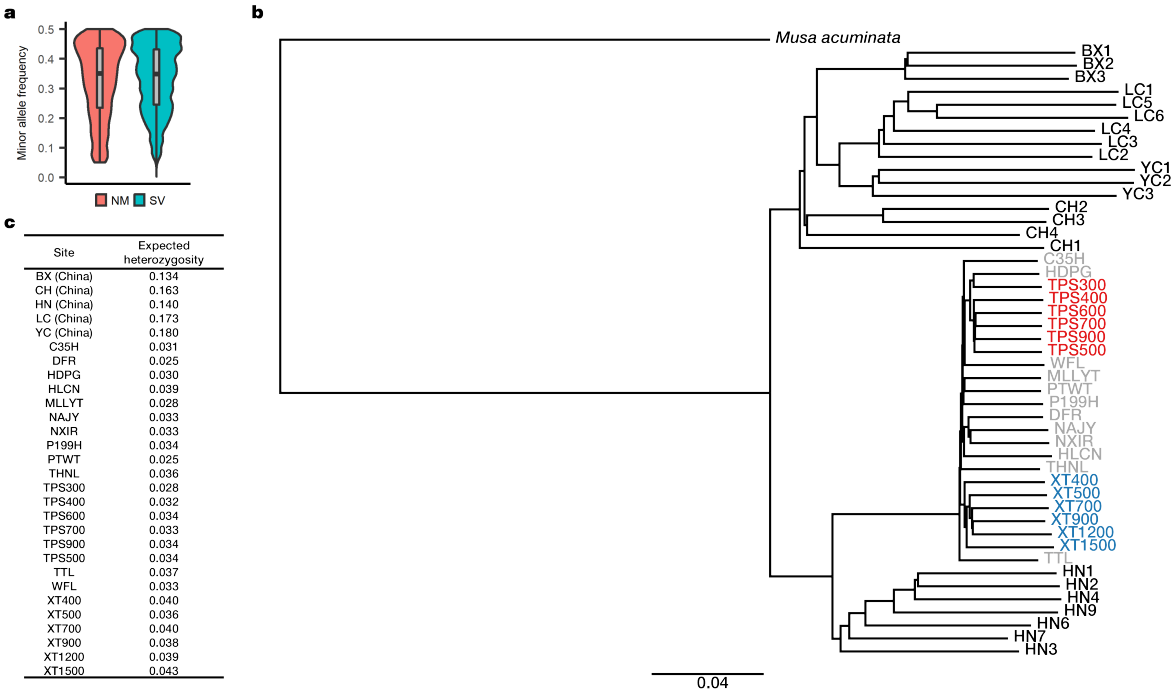

c

Site	Expected heterozygosity
BX (China)	0.134
CH (China)	0.163
HN (China)	0.140
LC (China)	0.173
YC (China)	0.180
C35H	0.031
DFR	0.025
HDPG	0.030
HLCN	0.039
MLLYT	0.028
NAJY	0.033
NXIR	0.033
P199H	0.034
PTWT	0.025
THNL	0.036
TPS300	0.028
TPS400	0.032
TPS600	0.034
TPS700	0.033
TPS900	0.034
TPS500	0.034
TTL	0.037
WFL	0.033
XT400	0.040
XT500	0.036
XT700	0.040
XT900	0.038
XT1200	0.039
XT1500	0.043

Supplementary Fig. 4 | Evolutionary analyses on Taiwanese and Chinese *Musa itinerans*. **a**, Minor allele frequency distribution of adaptive SNPs in Taiwan. **b**, Phylogeny of Taiwanese and Chinese *Musa itinerans*. The gray-colored indicates Taiwanese lowland populations (LE); the blue-colored indicates Taiwanese populations of Xitou transect (XT); the red-colored indicates Taiwanese populations of Taipingshan transect (TPS); the black-colored indicates Chinese accessions and the outgroup *Musa acuminata*. **c**, Table showing the expected heterozygosity among Taiwanese and Chinese populations.

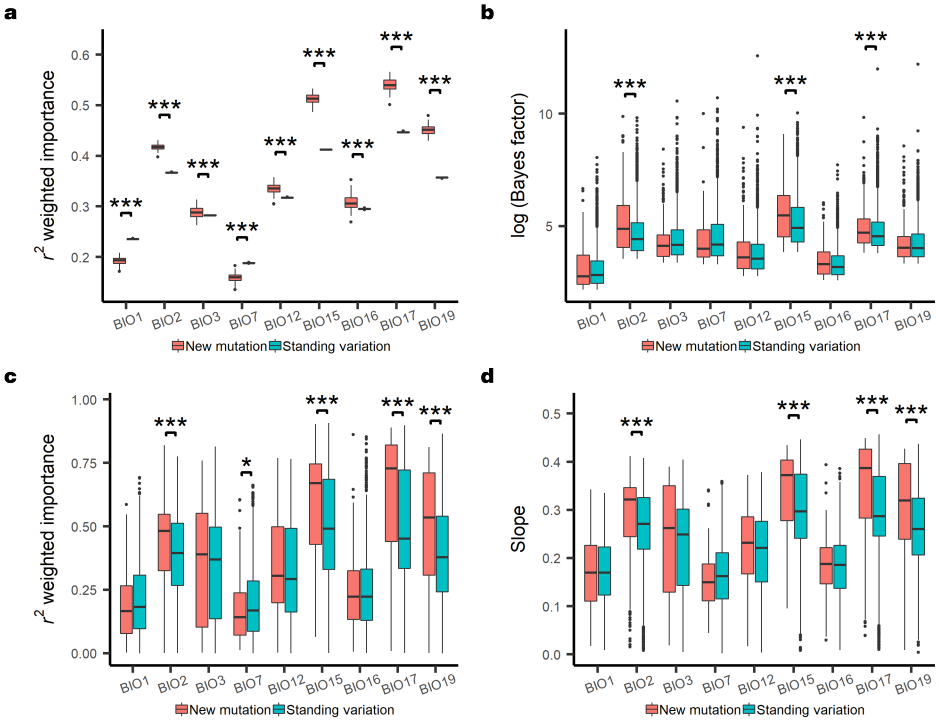

Supplementary Fig. 5 | Multi-analyses addressing ascertainment of standing variation and new mutation. a, The distribution of gradient forest r^2 importance across 100 re-sampling trials. In each re-sampling trials, a random set of 50% new mutations were assigned as standing variation, and the mean r^2 importance was reported for each trial. All comparisons show strong statistical significance from Student's *t*-test between new mutations and introduced standing variation (***$P < 0.001$). **b-d**, Profiling of effect sizes of adaptive SNPs with top 50% minor allele frequency. Distribution of Bayes factor (***$P < 0.001$, Wilcoxon rank-sum test; **b**), gradient forest r^2 importance (*$P < 0.05$, ***$P < 0.001$, Welch's *t*-test; **c**), and regression slopes of adaptive SNP allele frequency onto environmental gradients (***$P < 0.001$, Welch's *t*-test; **d**) is analyzed between new mutations and standing variation for each bioclimatic variable.

705 **Supplementary Table 1 | Population coordinates and bioclimatic information**

Site	Latitude	Longitude	BIO1	BIO2	BIO3	BIO7	BIO12	BIO15	BIO16	BIO17	BIO19
TPS300	24.60488	121.5359	208	63	35	180	2,970	46	1,223	364	364
TPS400	24.58135	121.5124	194	65	36	177	2,769	50	1,145	301	301
TPS500	24.56765	121.4992	199	65	36	179	2,763	50	1,142	299	299
TPS600	24.55172	121.5090	193	65	36	176	2,709	51	1,124	289	289
TPS700	24.54638	121.5125	185	65	37	174	2,699	49	1,107	302	302
TPS900	24.54021	121.5126	178	66	38	173	2,757	46	1,110	336	336
XT400	23.74292	120.7386	217	77	42	180	2,468	86	1,395	87	127
XT500	23.72780	120.7641	206	77	44	173	2,600	84	1,420	97	141
XT700	23.71137	120.7782	199	77	45	169	2,412	83	1,311	94	138
XT900	23.69294	120.7857	189	77	47	162	2,357	83	1,287	97	145
XT1200	23.67333	120.7854	176	77	48	159	2,478	82	1,346	97	148
XT1500	23.66936	120.7710	160	78	48	160	2,637	81	1,402	98	149
C35H	24.69907	121.1528	202	65	34	188	2,500	55	1,073	192	289
WFL	25.06752	121.7998	203	58	31	185	3,440	29	1,229	606	749
THNL	24.08273	120.8021	212	74	40	184	2,188	83	1,220	78	138
PTWT	22.58684	120.6489	227	78	49	158	2,912	98	1,784	79	87
P199H	22.24302	120.8465	223	73	50	144	3,114	92	1,856	178	178
MLLYT	24.33526	120.7864	211	71	37	190	2,056	76	1,084	79	148
HDPG	24.88347	121.5019	197	62	33	185	3,201	37	1,201	475	475
TTL	23.45230	120.6134	215	79	45	174	3,515	98	2,154	81	123
NAJY	24.43352	121.7602	216	62	35	174	2,860	61	1,328	271	296
HLCN	23.90623	121.4928	213	68	40	168	2,127	46	849	251	255
NXIR	23.40887	121.4503	227	71	43	163	2,147	57	938	211	211
DFR	23.10356	121.2724	206	75	48	155	2,017	68	1,026	166	166

706

707

708 **Supplementary Table 2 | SSR primer information**

Locus	Primer (5' to 3')	Chromosome*	Position*
CIR436	ATAAGCTCATATGGGTACAGTCACA CTGCAGCAACCAAATTTATTTCT	1	4,917,979 - 4,918,003 4,918,057 - 4,918,080
CIR276	CTCCTCCATAGCCTGACTGC TGACCCACGAGAAAAGAAGC	1	13,588,759 - 13,588,778 13,588,847 - 13,588,866
CIR1113	ACTCTCGCCCATCTTCATCC ACTTATTCCCCCGCACTCAA	1	28,009,948 - 28,009,967 28,010,173 - 28,010,192
Ma-3-132	TCCCTCTTCAACCAAAGCAC AACGCGAATGTGTGTTTTCA	2	20,365,901 - 20,365,920 20,366,041 - 20,366,060
CIR646	AACACCGTACAGGGAGTCAC GATACATAAGGCAGTCACATTG	2	23,940,966 - 23,940,985 23,941,276 - 23,941,297
Ma-1-17	AGGCGGGGAATCGGTAGA GGCGGGAGACAGATGGAGT	2	24,383,391 - 24,383,408 24,383,488 - 24,383,506
CIR332a	ATGACCTGTCGAACATCCTTT TCCCAACCCCTGCAACCACT	3	8,978,575 - 8,978,595 8,978,831 - 8,978,848
Ma-3-48	CCCGTCCCATTTCTCA TTCGTTGTTCATGGAATCA	5	32,672,883 - 32,672,898 32,673,018 - 32,673,036
CIR631a	ATTAGATCACCGAAGAACTC ATCTTTTCTTATCCTTCTAACG	6	33,942,751 - 33,942,770 33,943,017 - 33,943,038
CIR16a	TCATCTCACAATGCTTTCATAGTT TGGTTGAGTAGATCTTCTTGTGT	8	1,234,609 - 1,234,632 1,234,700 - 1,234,722
Ma-3-103	TCGCCTCTCTTTAGCTCTG TGTTGGAGGATCTGAGATTG	8	40,127,782 - 40,127,800 40,127,910 - 40,127,929
CIR348b	ACAGAATCGCTAACCCTAATCCTCA CCCTTTGCGTGCCCCTAA	10	27,228,162 - 27,228,186 27,228,325 - 27,228,342
Ma-3-139	ACTGCTGCTCTCCACCTCAAC GTCCCCCAAGAACCATATGATT	10	30,237,591 - 30,237,611 30,237,717 - 30,237,735
CIR550a	ACCGCACCTCCACCTCCTG TGCTGCCTTCATCGCTACTA	10	31,914,219 - 31,914,237 31,914,459 - 31,914,478

709

710 Primer sequences were searched against the *Musa acuminata* DH-Pahang version 2[33] on
711 Banana Genome Hub (https://banana-genome-hub.southgreen.fr/).
712 *The chromosome and position indicate locations on *Musa acuminata* where primer sequences
713 were found by blast.
714

715 **Supplementary Table 3 | Number of new-mutation (NM) or standing-variation (SV) SNPs**
716 **with (adaptive) or without (non-adaptive) significant associations with bioclimatic**
717 **variables**

Variable	Non-adaptive NM	Non-adaptive SV	Adaptive NM	Adaptive SV	*P*	Odds ratio
BIO1	293,348	954,367	816	7,113	8.92e-169	2.68
BIO2	293,274	953,198	890	8,282	8.43e-213	2.86
BIO3	293,551	953,901	613	7,579	6.47e-256	3.80
BIO7	293,644	953,981	520	7,499	1.32e-282	4.44
BIO12	293,452	954,272	712	7,208	3.12e-203	3.11
BIO15	293,168	951,447	996	10,033	2.33e-281	3.10
BIO16	293,826	957,605	338	3,875	1.95e-123	3.52
BIO17	293,461	954,969	703	6,511	1.61e-166	2.85
BIO19	293,516	955,326	648	5,142	1.06e-107	2.44

718
719 Statistical significance from χ^2 test is shown for each bioclimatic variable. Odds ratio is
720 calculated as (adaptive SV / adaptive NM) / (non-adaptive SV / non-adaptive NM).
721

722 **Supplementary Table 4 | Number of new-mutation (NM) or standing-variation (SV) SNPs**
723 **with (adaptive) or without (non-adaptive) significant associations with bioclimatic**
724 **variables (controlled for minor allele frequency)**

Variable	Non-adaptive NM	Non-adaptive SV	Adaptive NM	Adaptive SV	*P*	Odds ratio
BIO1	44,920	260,113	238	2,573	1.27e-20	1.87
BIO2	23,475	148,796	124	1,073	1.18e-03	1.37
BIO3	39,432	234,613	182	2,689	2.21e-34	2.48
BIO7	41,020	242,313	182	2,794	4.35e-38	2.60
BIO12	37,266	224,455	220	2,514	3.36e-20	1.90
BIO15	32,906	201,729	290	2,647	1.36e-10	1.49
BIO16	33,685	206,816	113	1,282	2.88e-10	1.85
BIO17	12,258	72,175	64	614	2.26e-04	1.60
BIO19	11,237	66,547	41	362	1.81e-02	1.50

725
726 The number of four sets of SNPs whose minor allele frequency (MAF) ranges from the first
727 quantile of adaptive MAF to the third quantile of non-adaptive MAF separately for each
728 bioclimatic variable is shown. Statistical significance from χ^2 test is shown for each
729 bioclimatic variable. Odds ratio is calculated as (adaptive SV / adaptive NM) / (non-adaptive
730 SV / non-adaptive NM).
731

732 **Supplementary Table 5 | Number of currently adaptive new-mutation (NM) or standing-**
733 **variation (SV) SNPs that remain (retention) or lose (disruption) significant associations**
734 **with environments under all future climate-change scenarios**

Variable	Disruption NM	Disruption SV	Retention NM	Retention SV	*P*	Odds ratio
BIO1	92	635	127	1,176	5.11e-02	1.30
BIO2	34	374	348	2,010	6.85e-04	0.53
BIO3	21	269	119	2,277	1.32e-01	1.50
BIO7	29	251	128	2,393	4.53e-04	2.20
BIO12	65	481	136	1,509	1.37e-02	1.50
BIO15	37	365	437	2,982	4.79e-02	0.69
BIO16	26	289	25	237	6.93e-01	0.85
BIO17	37	354	159	1,182	2.21e-01	0.78
BIO19	28	235	45	480	4.14e-01	1.30

735
736 Statistical significance from χ^2 test is shown for each bioclimatic variable. Odds ratio is
737 calculated as (retention SV / retention NM) / (disruption SV / disruption NM).